Contribution of nonthermodynamic processes to the formation of helium fragment in nucleus-nucleus collisions at 1.88*A* GeV

H. Fukshima, M. Miyagaki,* H. Fukushima,† C. Yokoyama, T. Hara, Y. Takahashi,†
T. Abe, and N. Hatani
Kobe University, Rokkodai, Nada, Kobe 657, Japan

C. Nagoshi
Institute for Nuclear Study, University of Tokyo, Tanashi, Tokyo 188, Japan
(Received 10 May 1990)

Exclusive-type experimental data on the emission of projectile helium fragments from the interactions of ^{56}Fe nuclei in the emulsion at 1.88*A* GeV (the dependence of angular distribution and mean multiplicity on the number of shower particles) are presented and discussed. The angular distribution is interpreted by simple superposition of well-known processes without assuming the existence of fireballs. In this paper, we present an interpretation on production of He fragments: *A* ^{4}He fragment is produced in a pickup process of a *p-n* pair by scattered *p-n* pair, and a ^{3}He fragment is produced by recombining a *p-n* pair and a proton that are scattered into small phase volume.

I. INTRODUCTION

Recently, much experimental effort has been devoted towards the investigation of relativistic nucleus-nucleus collisions with particular interest in the new collective phenomena, such as collective flow and phase transition, due to highly compressed nuclear matter [1–9]. Although a considerable amount of data [9–13] have resulted from the investigations, most of them could have no relation with the expected new phenomena because they were interpreted well simply in terms of a superposition of known proton-proton and/or proton-nucleus interactions. Possible indications of the interesting phenomena are, therefore, distinguished only by discriminating authentically collective processes from known ordinary process.

It seems that highly collective phenomena possibly appear in the collision of relativistic nucleus. In the emulsion experiments [14–19], which investigated the gross features of α fragment emission in the collision of heavy nuclei at the incident energy of the GeV/nucleon region, it has been commonly reported that the angular distribution of α fragments is reasonably fitted with a superposition of two functions derived from moving Boltzmann distributions. This fact has been interpreted as the result of α fragment emission from two kinds of thermodynamic sources, namely, hot and cool fireballs. The formation of cool fireball is probably understood by mechanisms similar to those at play in proton-nucleus interactions but that of hot fireball may be caused by highly collective and correlative mechanisms as pointed out by Baumgardt *et al.* [15].

It should be, however, noticed that there exists emission of helium fragments through a nonthermodynamic process (NTD) which consists of a few steps of ordinary interactions. In the collisions of light nuclei like ^{4}He, for example, helium fragments are emitted only through NTD because the number of nucleons involved in the collision system is too small to form a fireball state. In the collisions of heavy nuclei, the NTD is obviously never prohibited. On the contrary, it is uncertain whether or not the number of involved nucleons is enough to form thermal equilibrium. This means that the hypothesis of fireballs is not necessarily realistic even in the fragmentation of heavy nuclei. It is, therefore, interesting to investigate the contribution of NTD in the emission of helium fragments.

For this investigation, we can refer to the experimental data [19–22] on collision of light nuclei. Glagolev *et al.* investigated both elastic and inelastic interactions of ^{4}He nuclei with hydrogen target at an incident momentum of 8.56 GeV/*c* by 1-m bubble chamber at Dubna, and they presented the differential cross sections of various processes as functions of four-momentum transfer. Bizard *et al.* reported the data on angular dependence of ^{3}He production in the collisions of ^{4}He with proton at 6.85 GeV/*c* incident momentum using an achromatic double-focusing spectrometer at Saclay. The characteristic properties of NTD are expected to appear in these data.

In this article, we present exclusive-type data of emulsion experiments. In Sec. II, experimental procedures are described. Angular and multiplicity distributions of helium fragments are presented in Sec. III. In Sec. IV, the observed data are compared with those presented by Glagolev *et al.* [19] and Bizard *et al.* [21]. On the basis of the comparison, the contribution of NTD is estimated and the detailed mechanisms of NTD are also discussed.

II. EXPERIMENTAL PROCEDURES

Emulsion stacks were exposed to 1.88*A*-GeV Fe ions from BEVALAC at Lawrence Berkeley Laboratory (LBL 766-H experiment). Each stack was composed of 60 sheets of Fuji ET-7B emulsion pellicle which were prepared at Kobe University. The size of the pellicle is $2\times 10\times 0.06$ cm^3. The Fe beam was injected parallel to a 2-cm edge of pellicle with the density of about 3×10^3 ion/cm^2. After the beam exposure, five successive pellicles were stuck on the same backing Lucite plate connecting together at 10-cm edge and were processed. By this processing method, it was attained to reduce the regions to be excluded in data analysis due to edge distortion. Fiducial cuts were set at 1.5 mm from both upstream and downstream edges, 10 mm from side edge, and 10 μm from pellicle surface. The energy of incident Fe ion spreads down to 1.68A GeV by ionization loss in the fiducial volume.

Secondary charged particles emerging from observed interactions were classified into the following four groups: (1) Shower particles. The particles which have track with $I/I_0 \le 1.4$ where I and I_0 are the grain density of the concerned track and that of the singly charged plateau ionizing track, respectively. These particles are considered to be leading protons and secondary charged mesons. (2) Projectile helium fragments. The particles having track with $3.5 \le I/I_0 \le 4.5$ and $\theta \le 0.1$ rad, where θ is the emission angle referred to the incident beam track. (3) Projectile heavy fragments. The particles having track with $I/I_0 > 4.5$, and $\theta \le 0.1$ rad. (4) Target fragments. The particles having track with $I/I_0 > 1.4$, and $\theta > 0.1$ rad.

The statistical error of I/I_0 for a projectile helium fragment is 5.7% since the grain density has been measured over 300 μm. Accordingly, the missing probability of a projectile helium fragment due to this error is less than 3%. The misidentification probability of a slow proton, deuteron, triton, or pion as a projectile helium fragment is negligible because of the restriction of emission angle and ionization density.

For each event, the emission angles of helium fragments (θ_α), azimuthal angle of helium fragments referred to the emulsion surface (ϕ_α), the multiplicity of helium fragments (N_α), that of shower particles (n_s), that of projectile heavy fragments (N_f), and that of target fragments (N_h) were recorded.

θ_α of a fragment was calculated from the relative position of a point on the beam track, that on the fragment track, and that of the interaction vertex. For this measurement, semiautomatic systems of three coordinate digitized Nikon OPTIPHOTO microscopes with 2-μm read-out accuracy were used. In order to eliminate effects due to warping of the pellicle in stack and distortion in the processed emulsion, calculated values were corrected using the curvature of the nearby Fe beam track. The averaged accuracy of the corrected angular data is about 2 mrad and comparable to the beam divergence.

III. RESULTS

Out of 1783 minimum biased events obtained by along the track scanning, 1650 events located in the fiducial volume are selected for this analysis. The number of events with at least one helium fragment is 1297 and the total number of analyzed projectile helium fragments is 3030.

The number of events with each n_s, N_h, N_α, and N_f are listed in Table I. The average values of these multiplicities are 12.75, 11.44, 1.84, and 1.84, respectively. In the N_h distribution, one can observe three humps with peak at $N_h=0$, 4, and 20–25. This structure is considered to be caused by the target species.

Figure 1 shows the differential angular distribution ($dN/d\theta^2$) of all projectile helium fragments. The distribution can be fitted to a superposition of two exponential functions. The best-fitted functions are illustrated by

TABLE I. Number of events with each n_s, N_h, N_α, and N_f: $\langle n_s\rangle=12.75$, $\langle N_h\rangle=11.44$, $\langle N_\alpha\rangle=1.84$, and $\langle N_f\rangle=0.90$.

n_s	No. of events	n_s	No. of events	n_s	No. of events	N_h	No. of events	N_h	No. of events	N_h	No. of events	N_σ	No. of events	N_f	No. of events
0	19	19	50	38	1	0	192	16	26	32	14	0	353	0	424
1	24	20	46	39	3	1	97	17	26	33	15	1	452	1	991
2	51	21	35	40	2	2	64	18	42	34	10	2	349	2	220
3	53	22	43	41	1	3	120	19	39	35	16	3	254	3	14
4	73	23	39	42	2	4	133	20	25	36	7	4	145	4	0
5	105	24	24	43	2	5	107	21	24	37	10	5	60	5	0
6	93	25	30	44	1	6	99	22	37	38	9	6	23	6	1
7	88	26	11	45	0	7	61	23	30	39	2	7	0		
8	98	27	23	46	0	8	41	24	38	40	2	8	0		
9	78	28	19	47	0	9	35	25	35	41	4	9	1		
10	83	29	13	48	0	10	24	26	32	42	0				
11	86	30	4	49	0	11	23	27	16	43	0				
12	75	31	4	50	0	12	24	28	19	44	1				
13	67	32	5	51	1	13	26	29	24	45	1				
14	66	33	7	52	0	14	34	30	20	46	0				
15	52	34	6	53	0	15	26	31	20	47	0				
16	57	35	5	54	1										
17	47	36	2	55	0										
18	53	37	1	56	0										

dashed and dotted lines in Fig. 1(a). The χ^2/(degree of freedom) for this fitting is 27.52/15. The slope parameters of the fitted functions are $(11.4\pm0.7)\times10^2$ and $(1.7\pm0.5)\times10^2$, respectively. This result is consistent with those obtained by early experiments [14–18].

The shape of $dN/d\theta^2$ depends on shower particle multiplicity (n_s). The distribution for events classified with n_s is presented in Fig. 2; steep component decreases with n_s. The lines in the figure will be described in the next section.

The number of events with n_s and N_α are listed in Table II. The relation between mean multiplicity of projectile helium fragments ($\langle N_\alpha \rangle$) and multiplicity of shower particles (n_s) is shown in Fig. 3. The lines in the figure are also described in the next section.

IV. DISCUSSION

A. Angular distribution

As shown in Fig. 1(a), the differential angular distribution of all projectile helium fragments can be fitted with a superposition of two exponential functions. This fact seems to support the hypotheses of the "two fireball model" [14–16]. It should be, however, noticed that this distribution can be interpreted as the result of NTD.

The emission of helium fragment in the collisions of ^{4}He with hydrogen target is expected to be pure NTD because the number of nucleons involved in the collision system is too small to form a fireball state. Consequently, experimental data on such collisions permit us to find characteristic properties of NTD. As mentioned in Sec. I, a typical example of such experimental data has been reported by Glagolev *et al.* [19]. They presented differential cross sections of processes. (a) $^4\mathrm{He}+p\rightarrow{}^4\mathrm{He}+p$, (b) $^4\mathrm{He}+p\rightarrow{}^4\mathrm{He}+N+\pi$, (c) $^4\mathrm{He}+p\rightarrow{}^3\mathrm{He}(\text{spectator})+p+n$, (d) $^4\mathrm{He}+p\rightarrow{}^3\mathrm{He}+N(\text{spectator})+N$, as functions of four-momentum transfer, t or u, at a ^{4}He incident momentum of 8.56 GeV/c. They fitted their experimental points with exponential functions. The results of the fitting are summarized in Table III.

Concerning the emission of ^{4}He fragments in the collision of heavy nucleus, the processes similar to (a) and (b) probably take place. The former process is, however, suppressed because of low momentum transfer to the fragment. Experimental data in Ref. [19] indicate that less than 0.1% of scattered ^{4}He can get kinetic energy higher than 7 MeV/nucleon at the projectile rest frame. Most of the fragments scattered through the former process are, therefore, considered to be trapped by residual nucleus. On the other hand, there is no such suppression

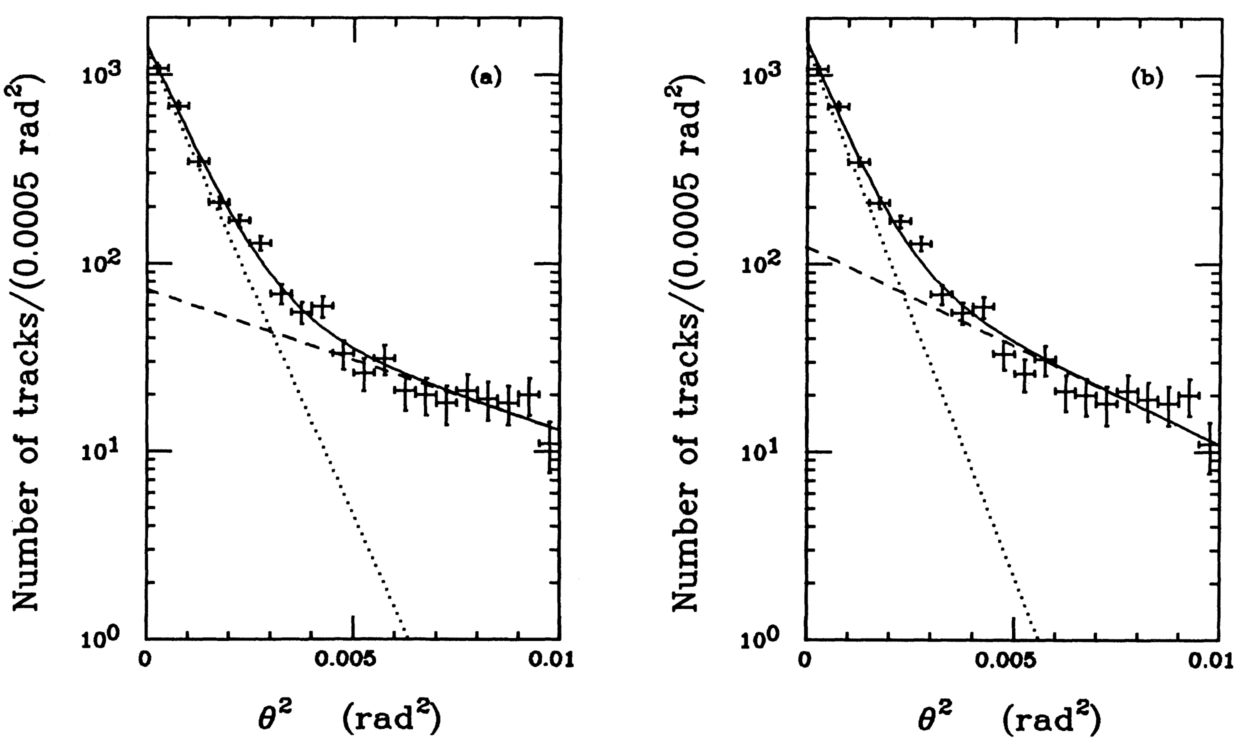

FIG. 1. Comparison of two kinds of fitting to the angular distribution. (a) Fireball fitting: Solid line is the best-fitted line with two exponential functions. The χ^2/(degree of freedom) for this fitting is 27.52/15. The slope parameters of the fitted functions are $(11.4\pm0.7)\times10^2$ and $(1.7\pm0.5)\times10^2$. Each parameter corresponds to dotted and dashed line. (b) NTD fitting: Solid line is the best fit due to the linear combination of Eqs. (2) and (4) (see text). Dashed and dotted lines illustrate ^{3}He and ^{4}He components, respectively. The χ^2/(degree of freedom) for this fitting is 32.25/17.

due to the momentum transfer in the latter process. Accordingly, it is reasonable to assume that the inelastic scattering similar to the process (b) is the dominant NTD for formation of ^{4}He fragments in high-energy heavy nucleus collisions.

Using the data listed in Table III, the differential frequencies of emitting ^{4}He (dN_4/dt) through this NTD are represented by the form

$$\frac{dN_4}{dt} \propto \exp(11.4t) . \quad (1)$$

In the case of this study, four-momentum transfer is approximated by $-p^2\theta^2$, where p is the momentum of the produced ^{4}He and is nearly equal to 10.6 GeV/c, so that we obtain the following expression for angular distribution of ^{4}He:

$$\frac{dN_4}{d\theta^2} = (1289)\kappa_4 \exp(-1289\theta^2) , \quad (2)$$

where κ_4 is the total number of ^{4}He.

The processes similar to (c) and (d) possibly contribute to the emission of ^{3}He in the collisions of heavy nucleus. It is, however, obvious that the former process is strongly suppressed because the transferred energy to the formed

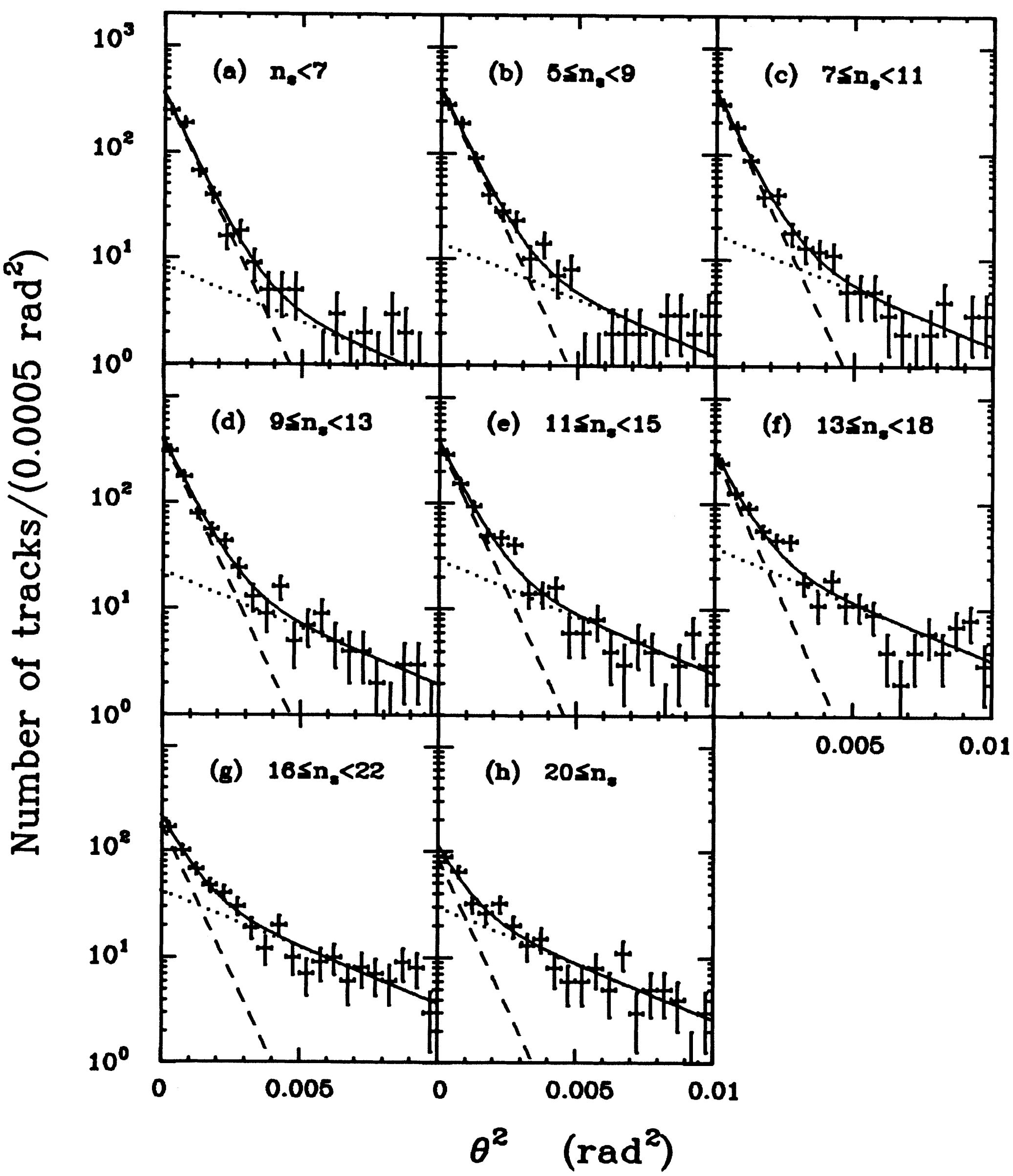

FIG. 2. Angular distributions for events classified with n_s: (a) $n_s < 7$, (b) $5 \le n_s < 9$, (c) $7 \le n_s \le 11$, (d) $9 \le n_s < 13$, (e) $11 \le n_s < 15$, (f) $13 \le n_s < 18$, (g) $16 \le n_s < 22$, (h) $20 \le n_s$. Dashed and dotted lines illustrate ^{3}He and ^{4}He components, respectively.

^{3}He is too low to eject it from the residual nucleus. The latter process consists of two different reactions. One is the coherent scattering of the three-nucleon system and another is the incoherent scattering, such as recombination of a proton and a p-n pair after scattering independently into small phase volume. The coherent scattering is also strongly suppressed because the scattered system scarcely gets enough momentum to leave the residual nucleus. In addition to this, the scattered system should be dissociated by the secondary scattering in the residual nucleus because the binding energy of a nucleon in ^{3}He is less than one-half of that in the heavy nucleus. On the

TABLE II. Number of events with n_s and N_α.

$ns/N\alpha$	0	1	2	3	4	5	6	7	8	9	Total	$\langle N\alpha \rangle$
0	6	10	2	1							19	0.89
1	8	12	3		1						24	0.92
2	17	24	4	3	1	2					51	1.08
3	7	28	12	5	1						53	1.34
4	15	27	16	11	3	1					73	1.49
5	21	30	30	16	3	3	1	1			105	1.70
6	18	30	22	13	6	4					93	1.69
7	24	25	16	14	5	2	2				88	1.60
8	8	23	23	18	17	5	2	2			98	2.47
9	12	19	19	12	10	5	1				78	2.10
10	8	27	19	14	7	5	1	2			83	2.17
11	11	20	15	17	11	5	3	4			86	2.51
12	5	14	20	12	13	7	3	1			75	2.69
13	8	13	16	11	11	4	3	1			67	2.49
14	2	15	15	17	10	4	1	1		1	66	2.70
15	3	6	17	13	7	3	2	1			52	2.71
16	9	13	13	8	11	1	2				57	2.18
17	5	12	10	8	8	3	1				47	2.32
18	5	13	10	16	6	3					53	2.26
19	11	14	13	7	4	1					50	1.64
20	5	14	11	13	3						46	1.89
21	8	8	7	8	3	1					35	1.80
22	13	12	9	7	2						43	1.37
23	13	12	8	4	1		1				39	1.28
24	13	5	3	2		1					24	0.92
25	13	8	8	1							30	0.90
26	4	3	2	2							11	1.18
27	14	6	2		1						23	0.61
28	13	3	3								19	0.47
29	10	2		1							13	0.38
30	3	1									4	0.25
31	3	1									4	0.25
32	4	1									5	0.20
33	7										7	0.00
34	5	1									6	0.17
35	5										5	0.00
36	2										2	0.00
37	1										1	0.00
38	1										1	0.00
39	3										3	0.00
40	2										2	0.00
41	1										1	0.00
42	2										2	0.00
43	1		1								2	1.00
44	1										1	0.00
51	1										1	0.00
54	1										1	0.00
57	1										1	0.00
Total	353	452	349	254	145	60	23	13	0	1	1650	1.84

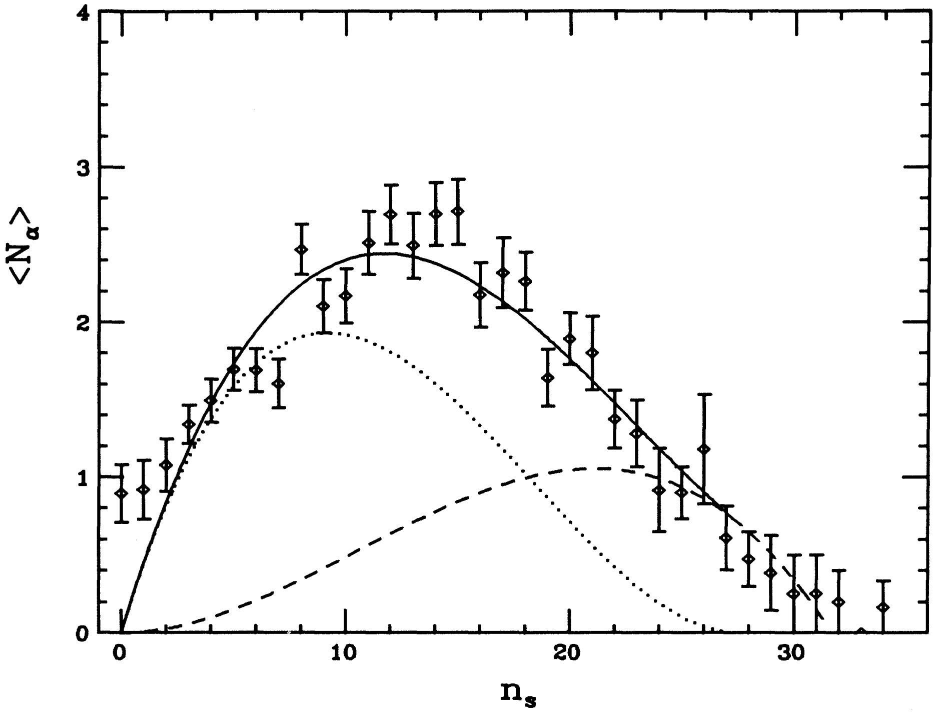

FIG. 3. Relation between mean multiplicitly of projectile helium fragments ($\langle N_\alpha \rangle$) and multiplicity of shower particles (n_s). Solid line represents the result of least-χ^2 fitting of observed $\langle N_\alpha \rangle$ with the function (14) (see text). The best values of ξ_4 and ξ_3 are $(6.19\pm0.20)\times10^{-4}$ and $(2.24\pm0.14)\times10^{-4}$, respectively. Dotted and dashed lines represent ^{4}He and ^{3}He components, respectively.

other hand, the recombination process is less suppressed though it is subject to the restriction of phase volume. Thus, we may assume that the recombination of proton and a p-n pair scattered into a small phase volume is the favorite NTD for producing ^{3}He in the collisions of heavy nucleus.

The data presented in Ref. [19] are not enough to obtain a reliable expression for angular distribution of ^{3}He formed through this NTD. But, we can refer to the data reported by Bizard *et al.* [21]. They investigated the angular distribution of the inclusive reaction $^4\text{He}+p \rightarrow {}^3\text{He}+X$ with 6.85-GeV/c incident alphas. The distribution is well fitted using a superposition of three exponential functions with slope parameters 3831 ± 581, 477 ± 14, and 101 ± 2.7. The functions are illustrated in Fig. 4. It is reasonable to assume that the components with these three slope parameters are produced through stripping of a neutron, coherent scattering of a three-nucleon system, and recombination of scattered p and p-n pair, respectively. As mentioned above, the first and the second components are strongly suppressed but the third component is favored in the collisions of heavy nucleus. Thus, we obtain the following expression for angular distribution of ^{3}He formed through dominant NTD at incident momentum of 6.85 GeV/c:

$$\frac{dN_3}{d\theta^2} \propto \exp(-101\theta^2) \ . \qquad (3)$$

Since the emission angle of projectile fragment is approximately proportional to the reciprocal of projectile momentum, the expression for the distribution at incident momentum of 10.6 GeV/c is given by

$$\frac{dN_3}{d\theta^2} = (243)\kappa_3 \exp(-243\theta^2) \ , \qquad (4)$$

where κ_3 is the total number of ^{3}He.

As shown in Fig. 1(b), our angular distribution is well fitted with the superposition of (2) and (4). The dashed and dotted lines in the figure illustrate ^{3}He and ^{4}He components, respectively. The χ^2/(degree of freedom) for this fitting is 32.15/17. This value is just the same as that obtained by the fitting based on the assumption of the two fireball model [solid line in Fig. 1(a)]. This result indicates that the fragmentation of Fe nuclei is completely explained by NTD. Formation of fireballs is, therefore, nothing but one of the possible assumptions to interpret the angular distributions.

In Figs. 2(a)–2(h), the results of least-χ^2 fitting of the angular distributions with the superposition of (2) and (4) for events classified with n_s are presented, respectively.

TABLE III. Slope parameters of exponential function fitted to t distribution (Ref. [19]), where t is the four-momentum transfer between the incident and outgoing ^{4}He.

Interaction	Slope parameter (GeV/c)$^{-2}$
$^4\text{He}+p \rightarrow {}^4\text{He}+p$	27.4 ± 1.5
$^4\text{He}+p \rightarrow {}^4\text{He}+N+\pi$	11.4 ± 1.9

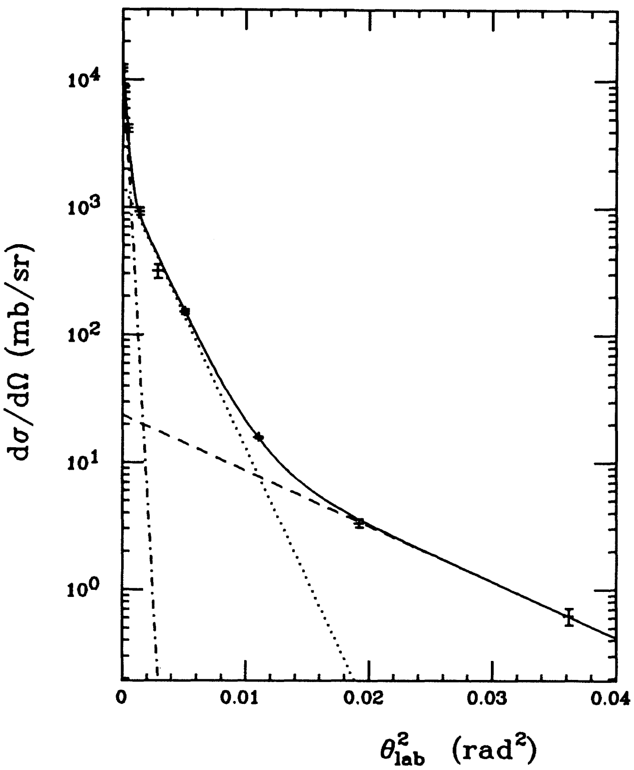

FIG. 4. Cross section of the inclusive reaction $^4He+p \rightarrow {}^3He+X$ with 6.85-GeV/c incident alphas (data Bizard *et al.* [21]). The data are fitted with three exponential functions (see text).

The dashed and dotted lines in the figures represent ^3He and ^4He components, respectively. The best values of κ_3 and κ_4 for each event sample are listed in Table IV. The ratio of ^4He to ^3He ($R=\kappa_4/\kappa_3$) vs n_s is presented in Fig. 5 by open squares.

The Fermi motion is considered to have influence on the angular distribution of emitted particles. Angular distribution of projectile helium fragments is well represented with a superposition of two Gaussian distributions, and the Fermi motion mainly effects on the width of the distribution. Therefore, the contribution of the Fermi motion to the angular distribution should be estimated before the advanced discussion on NTD.

Assuming that projectile helium fragments are emitted via NTD, slope parameters B_4 and B_3 are, respectively, related with the dispersions of distribution, σ_4^2 and σ_3^2, by the following formulas:

$$B_4=\frac{1}{2\sigma_4^2} \quad \text{and} \quad B_3=\frac{1}{2\sigma_3^2} ,$$

where $B_3=(243)$ and $B_4(=1289)$ are slope parameters obtained by He$+p$ experiments. The dispersions of the distribution should be larger due to the Fermi motion. This effect may differ with the species of emitted particles. Therefore, we can represent the effect as follows:

$$\sigma_4'^2=\sigma_4^2+\sigma_F^2 f_4 ,$$
$$\sigma_3'^2=\sigma_3^2+\sigma_F^2 f_3 , \qquad (5)$$

where the second term of the right-hand side is the correction term due to the Fermi motion. Using these relations, we get the following expression for angular distribution:

$$\frac{dN}{d\theta^2}=\kappa_4 B_4'\exp(-B_4'\theta^2)+\kappa_3\exp(-B_3'\theta^2) , \qquad (6)$$

where $B_4'=1/2\sigma_4'^2$ and $B_3'=1/2\sigma_3'^2$.

As described in Sec. III, the N_h distribution has three humps. Events in the first hump are produced by hydrogen target. Events in the second hump are produced by C, N, and O nuclei in the emulsion. And events in the third hump are produced by Br, Ag, etc. The largest effect of the Fermi motion is revealed for the heavier target. We may, therefore, estimate the effect by studying the angular distribution of the events with large N_h. For events with $N_h \geq 9$, the angular distribution is fitted with the expression (6). The fitting result does not show any meaningful difference for any value of f_4 and f_3. We assume, therefore, $f_4=f_3=1$. As the result, we get the dispersion due to the Fermi motion, $\sigma_F^2=(7.1\pm3.2)\times10^{-3}$.

Using this dispersion, we estimate the effect of the Fermi motion on the n_s dependence of the ratio of ^4He to ^3He. The ratio is calculated on the assumption that all events have this dispersion due to the Fermi motion. The assumption is considered to lead the overestimation of

TABLE IV. Values of κ_3 and κ_4 obtained from fitting the angular distribution $dN/d\theta^2=\kappa_3[243\exp(-243\theta^2)]+\kappa_4[1289.3\exp(-1289.3\theta^2)]$.

n_s	χ^2/N_{DF}	κ_4	κ_3	$\langle n_s \rangle$
Total	32.15/17	2143±58	1014±50	11.88
$n_s<7$	29.99/17	556±26	69±14	4.29
$5\leq n_s<9$	23.66/17	623±29	116±18	6.62
$7\leq n_s<11$	16.27/17	607±29	143±20	8.53
$9\leq n_s<13$	16.71/17	605±29	184±22	10.60
$11\leq n_s<15$	25.64/17	558±30	236±25	12.40
$13\leq n_s<18$	30.33/17	440±29	315±28	14.76
$16\leq n_s<22$	15.53/17	275±24	345±27	18.15
$20\leq n_s$	18.49/17	134±19	245±23	22.65

the Fermi motion. The result is also shown in Fig. 5 by open circles. The ratios are systematically different from the ratios represented by open squares. They are, however, consistent within one standard deviation. And, it does not give a serious effect on our final result.

B. Mean Multiplicity of helium fragment

The NTD discussed in Sec. IV A is considered to be originated from secondary collisions between recoiled target nucleons and residual projectile. The yields of fragments are, consequently, dependent on the number of recoiled nucleons (N_T) and the thickness of residual projectile (D). The dependence is regulated by the detailed mechanisms of the interaction processes. If the process is composed of a single-step interaction, the yield should be proportional to the number of recoiled nucleons and the effective thickness of residual projectile. In the case of successive two-step interaction, it should be proportional to the number of recoiled nucleons and the square of the effective thickness of the residue. And if the process is a recombination of two particles which are independently scattered into a small phase volume, it should be proportional to the squared number of recoiled nucleons and effective thickness of the residue.

The main formation process of ^{4}He [the process similar to (b) mentioned in Sec. IV A] is decomposed into several different combinations of subprocesses. Among the possible combinations, the single-step interaction is (b-1) coherent inelastic scattering of four-nucleon system expressed by

$$(pnpn)+N \rightarrow (NNN\mathcal{N})+N$$
$$\downarrow$$
$$^4\mathrm{He}+\pi \ ,$$

where $\mathcal{N}$ represents an excited state of a nucleon. This process is, however, suppressed since the momentum transfer is too low to eject the ^{4}He from residual nucleus.

Possible two-step interactions are the following, (b-2) and (b-3): (b-2) picking up of a p-n pair by another p-n pair inelastically scattered, namely,

$$(pn)+N \rightarrow (N\mathcal{N})+N$$
$$\downarrow$$
$$(N\mathcal{N})+(pn) \rightarrow {}^4\mathrm{He}+\pi \ ;$$

(b-3) recombination of two p-n pairs scattered into a small phase volume, namely,

$$(pn)+N \rightarrow (N\mathcal{N})+N$$
$$(pn)+N \longrightarrow (pn)+N$$
$$\downarrow$$
$$(N\mathcal{N})+(pn) \rightarrow {}^4\mathrm{He}+\pi \ .$$

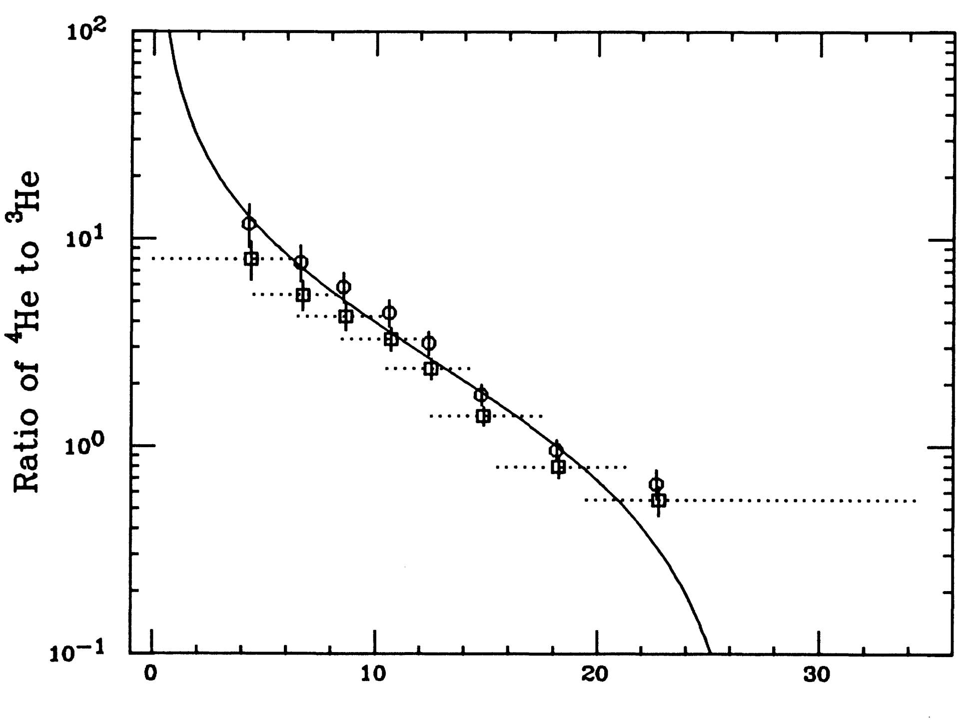

FIG. 5. Ratio of ^{4}He to ^{3}He ($R=\kappa_4/\kappa_3$) vs n_s obtained from the analysis of the angular distribution. Data points are plotted at average values of n_s of the region represented by dotted lines. Open squares represent the ratios obtained from the analysis based on the data of He+p experiments. Open circles represent the ratios obtained by taking the effect due to the Fermi motion into consideration. Solid line is the yield ratio of ^{4}He to ^{3}He for given n_s, i.e., $\langle N_4\rangle/\langle N_3\rangle$ as a function of n_s, obtained from the analysis of the multiplicity distribution.

The latter process is possible but unfavorable as compared with the former process because of the phase volume restriction.

As a matter of course, we may consider three- and more step interactions. Such interactions should be, however, suppressed because the occurrence probability of a multistep interaction drastically decreases with the number of subprocess. Thus, the process (b-2) is considered to be the most favorable in the production of ^{4}He fragments.

This process is forbidden unless two different p-n pairs are, at least, contained one behind another in the residual projectile. The minimum value of the thickness D required to produce ^{4}He fragments is, therefore, equal to the average thickness of ^{4}He. Hence, the effective thickness of residual projectile for this process is

$$D-(\tfrac{4}{3})4^{1/3} .$$

Taking this and the fact that the process is a successive two-step interaction into account, we obtain the following proportional expression for the production frequency of ^{4}He fragment in each event (i.e., mean multiplicity of ^{4}He fragment for given N_T):

$$\langle N_4 \rangle \propto N_T(D-(\tfrac{4}{3})4^{1/3})^2 . \tag{7}$$

The main process producing ^{3}He [the process similar to (d) mentioned in Sec. IV A] is also decomposed into several different combinations of subprocesses. Among the possible ones, the single-step interaction is (d-1) coherent scattering of three-nucleon system expressed by

$$(pnp)+N \rightarrow {}^3\mathrm{He}+N+(\pi) .$$

Two-step interactions are the following, (d-2) and (d-3): (d-2) picking up of a p-n pair (or proton) by another proton (or p-n pair) scattered, namely,

$$\begin{array}{l}(pn/p)+N \rightarrow (pn/p)+N+(\pi) \\ \qquad\qquad\qquad\quad \downarrow \\ \qquad\qquad\qquad (pn/p)+(pn/p) \rightarrow {}^3\mathrm{He} ;\end{array}$$

(d-3) recombination of a proton and a p-n pair scattered into small phase volume, namely,

$$\begin{array}{l}(pn)+N \rightarrow (pn)+N+(\pi) \\ \quad N+N \longrightarrow \big| \rightarrow p+N+(\pi) \\ \qquad\qquad\qquad \downarrow \qquad \downarrow \\ \qquad\qquad\qquad (pn)+p \rightarrow {}^3\mathrm{He} .\end{array}$$

Since the binding energy of nucleon in a ^{3}He is less than one-half of that in a heavy nucleus, the ^{3}He formed through the process (d-1) or (d-2) should be dissociated before it leaves the residual projectile. Emission of ^{3}He through these processes is, therefore, strongly suppressed. On the other hand, the ^{3}He formed through the process (d-3) cannot be broken because the recombination of the scattered particles may take place after they left the residue. Hence, we may assume that the process of (d-3) dominates in the formation of ^{3}He in the collision of heavy nuclei though it is subject to the restriction of phase volume as mentioned in Sec. IV A.

This process is allowed if a proton and a p-n pair are contained side by side in the residual projectile. The minimum value of D required to produce ^{3}He is, therefore, equal to the average thickness of ^{2}H. From this, the effective thickness of residual projectile for production of ^{3}He is estimated to be

$$D-(\tfrac{4}{3})2^{1/3} .$$

Taking this and the fact that the process is a recombination of two particles into consideration, we obtain the following proportional expression for the production frequency of ^{3}He fragment in each event (i.e., mean multiplicity of ^{3}He fragment for given N_T):

$$\langle N_3 \rangle \propto N_T^2[D-(\tfrac{4}{3})2^{1/3}] . \tag{8}$$

In the case of this study, N_T can be estimated from n_s since the number of primary nucleon-nucleon interactions is roughly equal to N_T. The relation between n_s and n_T is approximately given by

$$n_s=\left[\frac{Z_p}{A_p}+\frac{2}{3}\langle N_\pi \rangle \frac{\sigma_{\mathrm{inel}}(pp)}{\sigma_{\mathrm{tot}}(pp)}\right]N_T , \tag{9}$$

where $\sigma_{\mathrm{inel}}(pp)/\sigma_{\mathrm{tot}}$ is the ratio of the inelastic cross section to the total cross section of pp collision, $\langle N_\pi \rangle$ is the mean pion multiplicity in an elastic pp collision, and Z_p/A_p is the ratio of atomic number to mass number of the projectile. Substituting known numerical values into (6), we obtain

$$N_T=1.18n_s . \tag{10}$$

The value of D can be also related to n_s since the number of nucleons involved in the residual projectile is equal to A_p-N_T. If the nucleon radius to taken as the unit of length, the volume and approximated cross section of residual projectile are estimated to be $\frac{4}{3}\pi(A_p-N_T)$ and $\pi A_p^{2/3}$, respectively. Hence, the averaged value of D for a certain value of N_T is represented by

$$D(N_T)=\tfrac{4}{3}A_p^{-2/3}(A_p-N_T) . \tag{11}$$

Substituting the relations (10) and (11) into (7) and (8), we obtain the expressions

$$\langle N_4 \rangle \propto n_s(27.7-n_s)^2 \tag{12}$$

and

$$\langle N_3 \rangle \propto n_s^2(31.7-n_2) , \tag{13}$$

respectively. The mean multiplicity of projectile helium fragment for a given n_s is, therefore, given by the linear combination of (12) and (13), namely,

$$\langle N_\alpha \rangle = \xi_4 n_s(27.7-n_s)^2+(\xi_3 n_s^2(31.7-n_s) . \tag{14}$$

The solid line in Fig. 3 represents the result of least-χ^2 fitting of observed $\langle N_\alpha \rangle$ with the function (14). The fitting is sufficiently good. The best values of ξ_4 and ξ_3 are $(6.19\pm0.20)\times10^{-4}$ and $(2.24\pm0.14)\times10^{-4}$, respectively. Dotted and dashed lines in the figure represent ^{4}He and ^{3}He components, respectively. The overall fraction of ^{4}He is estimated to be $(70.5\pm1.7)\%$ from this fitting result. The yield ratio of ^{4}He to ^{3}He for given n_s, i.e., $\langle N_4 \rangle / \langle N_3 \rangle$ as a function of n_s, is also estimated from this result. The estimated ratio is illustrated in Fig. 5 by the solid line. The ratio completely agrees with that obtained from the analysis of θ^2 distributions. It should be emphasized that these ratios result from essentially independent data analyses. Excellent agreement between these ratios, therefore, indicates the reasonability of our assumptions employed here.

Figure 5 also indicates that the production of ^{4}He dominates the collisions with light target and peripheral collisions with heavy target while the production of ^{3}He dominates in close collisions with heavy target.

V. CONCLUSIONS

We have obtained exclusive-type data on the emission of projectile helium fragment in the nucleus-nucleus collisions at 1.88A-GeV incident energy from the study of 1783 minimum biased events of ^{58}Fe interaction in photographic emulsion. We have investigated the contribution of NTD to the emission mechanisms of ^{3}He and ^{4}He using the data, particularly the dependence of angular distribution and mean multiplicity on the number of shower particles. The conclusions are as follows.

(1) Angular distribution of projectile helium fragments is completely explained only by superposition of well-known nonthermodynamic processes (NTD), namely, the similar processes as

$$^4\text{He}+p \rightarrow {}^4\text{He}+N+\pi$$

and

$$^4\text{He}+p \rightarrow {}^3\text{He}(\text{incoherent})+N(\text{spectator})+N+(\pi),$$

without assuming the existence of fireballs.

(2) It is reasonable to assume that ^{4}He fragment is produced in pickup process of a p-n pair by scattered p-n pair, and that ^{3}He fragment is produced in recombination of a p-n pair and a proton which are scattered into small phase volume. Under these assumptions, the mean multiplicity of helium fragment for given n_s is represented by a cubic expression,

$$\langle N_\alpha \rangle = [6.19 n_s (27.7 - n_s)^2 + 2.24 n_s^2 (31.7 - n_s)] \times 10^{-4} .$$

The first and the second terms of the right-hand side correspond to ^{4}He and ^{3}He components, respectively. Observed data are reproduced by this equation well.

(3) The yield ratio of ^{4}He to ^{3}He for a given n_s is estimated by two independent methods. One is based on the analysis of angular distributions and another is based on that of mean multiplicity. The results of these estimations excellently agree with each other.

Putting all these results together, it is supposed that hot and cool α fragments in the "two fireball model" are misunderstanding of ^{3}He and ^{4}He emitted through NTD. It should be, however, noticed that these results do not exclude completely the possibility of fireball formation. Since the θ^2 distribution in the NTD bears close resemblance to that expected from the assumptions of fireballs, it is impossible to distinguish NTD from fireball formation without exclusive analyses, especially the momentum of each helium fragment over the whole p_T range.

ACKNOWLEDGMENTS

The authors would like to thank Professor O. Hashimoto for his fruitful comments and discussion. One of the authors (H.F.) thanks Dr. H. Hamagaki for his hospitality.

*Present address: Himeji Dokkyo University, Kamiohno, Himeji 670, Japan.
†Present address: Osaka University of Commerce, Higashi-Osaka 577, Japan.

[1] H. Stöcker, J. A. Maruhn, and W. Greiner, Phys. Rev. Lett. **44**, 725 (1980).
[2] H. Stöcker *et al.*, Phys. Rev. Lett. **47**, 1807 (1981).
[3] H. A. Gustafsson *et al.*, Phys. Rev. Lett. **52**, 1590 (1984).
[4] R. Stock *et al.*, Phys. Rev. Lett. **44**, 1243 (1980).
[5] R. Stock *et al.*, Phys. Rev. Lett. **49**, 1236 (1982).
[6] P. J. Siemens and J. O. Rasmussen, Phys. Rev. Lett. **42**, 880 (1979).
[7] G. Buchwald, G. Graebner, J. Theis, J. Maruhn, and W. Greiner, Phys. Rev. Lett. **52**, 1594 (1984).
[8] H. G. Baumgardt, J. U. Schott, Y. Sakamoto, E. Schopper, H. Stöker, J. Hofmann, W. Scheid, and W. Greiner, Z. Phys. A **273**, 359 (1975).
[9] Y. P. Viyogi *et al.*, Phys. Rev. Lett. **42**, 33 (1979).
[10] J. Gosset *et al.*, Phys. Rev. C **16**, 629 (1977).
[11] S. Nagamiya, L. Anderson, W. Brückner, O. Chamberlain, M.-C. Lemaire, S. Schnetzer, G. Shapiro, H. Steiner, and I. Tanihata, Phys. Lett. **81B**, 147 (1979).
[12] A. Sandoval *et al.*, Phys. Rev. C **21**, 1321 (1980).
[13] S. Nagamiya, M. C. Lemaire, E. Moeller, S. Schnetzer, G. Shapiro, H. Steiner, and I. Tanihata, Phys. Rev. C **24**, 971 (1981).
[14] H. H. Heckman, D. E. Greiner, P. J. Lindstrom, and H. Shwe, Phys. Rev. C **17**, 1735 (1978).
[15] H. G. Baumgart, E. M. Friedländer, and E. Schopper, J. Phys. G **7**, L175 (1981).
[16] T. Hasegawa, S. Tasaka, Y. Sato, H. Sugimoto, K. Taira, and N. Takeyama, J. Phys. Soc. Jpn. **54**, 3289 (1985).
[17] K. B. Bhalla *et al.*, Nucl. Phys. **A367**, 446 (1981).
[18] M. M. Aggarwal, K. B. Bhalla, G. Das, and P. L. Jain, Phys. Rev. C **27**, 640 (1983).
[19] V. V. Glagolev *et al.*, Phys. Rev. C **18**, 1382 (1978).
[20] V. V. Glagolev *et al.*, Nucl. Phys. **A445**, 572 (1985).
[21] G. Bizard *et al.*, Nucl. Phys. **A285**, 461 (1977).
[22] J. Banaigs *et al.*, Phys. Rev. C **35**, 1416 (1987).